Hydrol. Earth Syst. Sci. Discuss., 9, 7181–7225, 2012
www.hydrol-earth-syst-sci-discuss.net/9/7181/2012/
doi:10.5194/hessd-9-7181-2012

Hydrology and
Earth System
Sciences
Discussions

Thermal management of an urban groundwater body

J. Epting and P. Huggenberger

Department of Environmental Sciences, Applied and Environmental Geology, University of Basel, Bernoullistr. 32, 4056 Basel, Switzerland

Received: 24 April 2012 – Accepted: 22 May 2012 – Published: 6 June 2012

Correspondence to: J. Epting (jannis.epting@unibas.ch)

Published by Copernicus Publications on behalf of the European Geosciences Union.

Abstract

This study presents a management concept for the sustainable thermal use of an urban groundwater body. The concept is designed to be applied for shallow thermal groundwater use and is based on (1) a characterization of the present thermal state of the investigated urban groundwater body; (2) the definition of development goals for specific aquifer regions, including future aquifer use and urbanization; and (3) an evaluation of the thermal use potential for these regions.

The investigations conducted in the city of Basel (Switzerland) focus on thermal processes down-gradient of thermal groundwater use, effects of heated buildings in the aquifer as well as the thermal influence of river-groundwater interaction. Investigation methods include: (1) short- and long-term data analysis; (2) high-resolution multilevel groundwater temperature monitoring; as well as (3) 3-D numerical groundwater flow and heat-transport modeling and scenario development. The combination of these methods allows quantifying the thermal influence on the investigated urban groundwater body, including the influences of thermal groundwater use and additional heat from urbanization. Subsequently, management strategies for minimizing further groundwater temperature increase, targeting "potential natural" groundwater temperatures for specific aquifer regions and exploiting the thermal use potential are discussed.

1 Introduction

Thermal groundwater regimes in urban areas are affected by numerous anthropogenic changes, as surface sealing or subsurface constructions as well as groundwater use. Additionally, the extension of subsurface infrastructures and the diffuse heat input of heated buildings have resulted in elevated groundwater temperatures observed in many urban areas (e.g. Taniguchi et al., 1999, 2007; Ferguson and Woodbury, 2004; Epting et al., 2011; Zhu et al., 2010, 2011). Also in Northwestern Switzerland, Basel, groundwater temperatures have increased significantly, and have reached up to 17 °C in an area where the long-term average annual air temperature is approximately 10 °C. This increase is substantial, considering the groundwater temperatures in areas not influenced by anthropogenic activities should be comparable to the average annual air temperature.

Prediction of groundwater temperatures is an important issue for groundwater management in urban areas (Florides and Kalogirou, 2007; Pouloupatis et al., 2011; Shi et al., 2008). In particular when considering the missing rules for resource management in urban areas as well as current deficiencies in adaption strategies related to future environmental development and mitigation measures for infrastructures.

Therefore, understanding groundwater heat transport is essential for the design, performance analysis and impact assessment of thermal devices (e.g., Fujii et al., 2005). The design and construction of shallow geothermal systems has been investigated comprehensively. Spitler (2005) reviewed past ground-source heat pump system research, from the 1940s to present and Kalogirou and Florides (2007) provide a comprehensive review of geothermal systems. The main issues are: (1) How can production temperatures (cooling or heating) be maintained throughout the years? (2) How far extents the area influenced by cooling or heating around the injector (Banks, 2009)?

Evaluating the effect of geothermal systems on subsurface environments requires appropriate monitoring and modeling tools. Recent availability of simple and reliable temperature measurement devices and the advancement of 3-D heat transport models facilitate investigations of subsurface heat transport at different scales. Fujii et al. (2007) proposed the development of suitability maps for the Chikushi Plain (Western Japan) based on local geological and hydrogeological information for ground-coupled heat pump systems using field-survey data and numerical groundwater and heat transport models. Zhu et al. (2010, 2011) evaluated the case-specific potential heat content in urban aquifers and quantified available capacities for space heating. Detailed groundwater temperature measurements in Cologne (Germany) and Winnipeg (Canada) reveal high subsurface temperature distributions in the centers of both cities and indicate a warming trend of up to 5 K. Such geothermal potentials are also observed in other cities such as Shanghai and Tokyo and can supply heating demand even for decades. Also Allen et al. (2003) propose that Northern European countries can utilize the urban heat island effect to generate low enthalpy geothermal energy for space heating and cooling systems (dual heating and cooling functions) in buildings, provided a suitable aquifer underlies the urban area.

Dahlem and Heinrich (1999) and Dahlem (2000) investigated the influence of groundwater flow on the heat-loss of heated cellars. They found, that heat-loss due to advective groundwater flow can be in the order of 10 times higher compared to solely conductive heat-loss. Ampofo et al. (2006) reviewed groundwater cooling systems in London. They show that environmental influence of building parts that reach into the groundwater has increased the pressure on architects, engineers and building operators to reduce the use of air conditioning in favor of more passive cooling solutions. However, the proposed solutions are limited to new-build projects.

Currently, in most urban areas, regulations for water resource management and geothermal energy use are sparse and limited to the rule “first come, first served”. Also in urban areas, groundwater-based heating and (especially) cooling schemes are being planned, sometimes with minimal hydrogeological input (Banks, 2009). Haehnlein et al. (2010) compiled the international status of the use of shallow geothermal energy. Commonly, groundwater temperature changes are restricted by installation guidelines or occasionally by governmental environmental agencies. For instance, in Switzerland, the maximum allowed temperature difference induced from geothermal energy use is 3 K down-gradient of thermal groundwater use in relation to a “natural state” of groundwater temperatures without anthropogenic influence (GSchV, 2001).

This study presents strategies for the thermal management of urban groundwater and how to predict the influence of thermal systems and urban subsurface development on the basis of field-scale geological and hydrological data as well as 3-D numerical groundwater flow and heat-transport modeling and scenario development. A concept for adaptive resource management and shallow thermal groundwater use in the investigated urban area is presented, which is based on the characterization of the present

Title Page
Abstract | Introduction
Conclusions | References
Tables | Figures
◀◀ | ▶▶
◀ | ▶
Back | Close
Full Screen / Esc
Printer-friendly Version
Interactive Discussion

thermal state of the urban groundwater body (GWB) (CEC, 2000). This includes the description of groundwater flow and thermal regimes as well as a classification of unaffected, temporary or continuous temperature influences.

Several factors affecting the magnitude and timing of temperature increases and decreases are examined, with focus on: (1) thermal groundwater use for cooling purposes; (2) the effect of heated buildings reaching into the aquifer, with emphasis on building density and the urban heat island effect; and (3) the role of river-groundwater interaction affecting riverine temperature patterns in the aquifer.

A set of scenarios is presented that focuses on the compensation of past influences on the thermal groundwater regime such as thermal groundwater use and urbanization. For specific aquifer regions thermal groundwater use is simulated where groundwater is used for heating purposes and cool water is reinjected back into the aquifer. As a result groundwater temperatures down-gradient return to “potential natural” values observed in uninfluenced aquifer regions. Subsequently, the sustainability of such approaches is investigated.

2 Settings

Many Swiss valleys which are underlain by unconsolidated alluvial sediments belong to the most densely populated areas. Furthermore, these aquifers are important for drinking and process water supplies and as they maintain a relatively stable geothermal source or sink the aquifers are suited for the geothermal use of groundwater.

The investigated shallow unconfined aquifer in the Basel area consists of late Pleistocene gravels deposited by the river Rhine. The thickness of the aquifer ranges between 15 and 27 m and is underlain by an aquiclude consisting of mud to clay rich sediments, Oligocene in age.

The area covers business and residential districts, industrial areas and green spaces. Parts of the investigated area formerly were contaminated by industrial activities (Epting et al., 2008a). A total of 13 industrial wells are operated, the average amount of groundwater extracted from the aquifer is about 30 $\mathrm{l\,s^{-1}}$, and approximately 3.5 $\mathrm{l\,s^{-1}}$ is injected back to the aquifer (Fig. 1). Cooling using groundwater has gained popularity in recent years. Among the reasons for this are the excellent energy efficiency and the increasing viability of water extraction systems. For groundwater cooling systems cold water is abstracted from one part of the aquifer system (the "cold" well; typically at 6–12 °C, depending on the aquifer and location) and is used via a heat exchanger for cooling the building. The resultant heated water is then recharged into the aquifer at a different location (the "hot" well). As in the city of Basel a heating network already exists, groundwater currently only is used for cooling purposes.

Although many newer buildings have insulated basements, this is a relatively new practice and a significant amount of heat loss will have already occurred within the investigated area. It also has to be considered that Basel is a fairly old city when compared e.g. to many cities in Northern America. Next to building parts that reach into the aquifer also further constructions lie within the aquifer; this includes a 3.2 km long subsurface highway that partly lies within the aquifer perpendicular to the main groundwater flow direction as well as a 550 m long sheet pile wall at the river board (Fig. 1).

The groundwater regime of the area has already been investigated intensively in the scope of various stresses on the GWB during the construction of a tunnel highway in the northwestern area of Basel, Switzerland (Epting et al., 2008a, b). The main direction of the regional groundwater flow is from south to north and from west to east (Fig. 1). A steep gradient of the hydraulic heads in the middle of the model area coincides with a steep slope of the bedrock surface in this area (Figs. 1 and 2). By contrast, comparatively low hydraulic gradients and groundwater velocities in the northern industrial area behind the sheet pile wall on the river board can be observed (see below; Fig. 1).

3 Methods

3.1 Monitoring groundwater temperatures in space and time

Within the investigated GWB a total of 27 observation wells for continuous measurements of the hydraulic head and groundwater temperature is run by the Agency for Environment Basel-Stadt (AUE BS). A preliminary analysis of existing temperature time-series revealed that meaningful data interpretation is difficult. Possible reasons for this shortcoming are assumed to be caused by the non-uniformity in the construction of the conventional observation wells as well as missing information, including: (1) the vertical position of the temperature sensor within the observation well; (2) the position of the observation wells' screen within the flow field; (3) the consideration of the infiltration of surface waters; (4) the sensitivity concerning changes within the regional groundwater flow regime; (5) groundwater usage; and (6) possible measurement errors.

In order to make more reliable interpretations of groundwater temperature distributions four multilevel observation wells were installed (Fig. 1) which provide continuous temperature measurements at discrete points vertically within the aquifer at 0.5 to 1 m depth intervals. Thermistor thermometers were used, which can read temperature at 0.01 K accuracy. As the screening sections were either separated or entirely filled by bentonite no thermal free convection was expected. The multilevel observation wells focus on capturing several processes, as: (I) river-groundwater interaction effects on thermal groundwater regimes; (II) influence of thermal groundwater use on the thermal groundwater regime down-gradient; and (III) effects of building parts reaching into the aquifer and their down-gradient influence on thermal groundwater regimes, including seasonal heating phases. Additionally, a fourth (IV) device for multilevel temperature monitoring was installed for defining the southern model boundary.

The skin effect for the boreholes of the new measurement devices was numerically evaluated by synthetic models. According to Barrash et al. (2006) wellbore skin causes either an additional resistance to flow (positive skin) if it has lower hydraulic conductivity than the undisturbed formation (e.g. invasion of drilling mud into the formation;

encrustation or sand-clogging of the well screen), or causes a lessened resistance to flow (negative skin) if it has higher hydraulic conductivities than the disturbed formation (e.g. sand or gravel pack in annular space). It could be verified through synthetic modeling experiments that the temperature on the inside wall of the observation wells tube equilibrated rapidly with the temperature on the outside of the wall.

The head and temperature of the river Rhine is measured at three locations by the Federal Office for the Environment, Switzerland (FOEN) and the AUE BS. The mean annual river water temperature for the period 1995 to 2009 was 12.7 °C; the maximum and minimum river water temperatures for this period were 26.2 °C and 3.1 °C, respectively.

3.2 Set-up and calibration of the heat-transport model

The movement of thermal plumes through the subsurface is controlled by groundwater velocity and thermal properties of the aquifer. Physical processes affecting heat transport within an aquifer include advection, dispersion and diffusion. The diffusion of heat depends on the thermal conductivity and volumetric heat capacity of the aquifer. In a composite medium, such as an aquifer, the properties of both the fluid and the solid phase of the porous media have to be considered. For the exchange and heat transfer between the aquifer system with the upper boundary (e.g. from the atmosphere or through the unsaturated zone) or surface waters (e.g. rivers, lakes) a transfer coefficient is required (see below).

For the present study the flow and heat-transport models were set up in FEFLOW© (Diersch, 2002) and have been calibrated for the time series of 2010 (27 observation wells with head and temperature data). Furthermore, the temperature measurements of the multilevel observation wells were used to further calibrate the model. The area covers 2720 m × 2860 m (about 8 km^2; Figs. 1 and 2). The aquifer base includes the information of more than 400 drill-cores and was modeled using GoCAD© (Geological Objects Computer Aided Design). GOCAD is an integrated 3-D geologic object modeling and visualization software application. The software is based on a discrete smooth interpolation (DSI) algorithm (Mallet, 1992, 2002).

Values for thermal conductivity and heat capacity for the porous media and groundwater were derived from the literature (Table 1). Markle et al. (2006) characterized the two-dimensional thermal conductivity distribution in a sand and gravel aquifer and provide values for thermal conductivities for glacial soils. Otto (2010) compiled thermal conductivities of shallow unconsolidated rock for Northern Germany. Fluid viscosity dependencies were incorporated choosing the standard settings in FEFLOW© using an empirical relationship as can be found in the literature (Lever and Jackson, 1985; Hassanizadeh, 1988).

17 layers were integrated to adequately include the measurement levels of the multilevel temperature sensors. A thickness of 0.5 m for the lower layers was distributed uniformly from the basement; the uppermost layer reaches up to the surface and includes the unsaturated zone. The topography was derived from a DEM with 25 m resolution and high-precision echo sounding of the river bed. The resulting volume of the 3-D groundwater model amounts to $1.45 \times 10^9\ \mathrm{m}^3$. Building parts that reach into the aquifer, including a sheet pile wall at the river board and a tunnel road, were considered as regions with very low hydraulic conductivities. The effect of lost heat from the canalization and the district heating network was neglected as these objects mainly lie in the unsaturated zone (Fig. 2).

The distribution of horizontal hydraulic conductivity zones is based on data sets from pumping tests and drill-core descriptions which were available from the geological database developed by the Applied and Environmental Geology of the University of Basel (GeoData, Epting et al., 2008a, b) as well as considerations of fluvial depositional processes. The ratio of horizontal to vertical hydraulic conductivity as well as the ratio of longitudinal to transversal dispersivity is assumed to be 10. A porosity of 0.12 and a longitudinal dispersivity of 20 m were derived from regional field studies, including results from dye tracer tests.

In order to adequately discretize the time-varying thermal and hydraulic boundary condition of the river Rhine daily time intervals of temperature and head data were chosen. An initial distribution of groundwater head and temperature were interpolated on the basis of measured head and temperature data in the observation wells. In the following the model boundaries for flow and thermal transport (sources and sinks) are defined.

3.2.1 Calculation of areal groundwater recharge by percolating meteoric water

Areal groundwater recharge by percolating meteoric water is based on meteorological data derived from the Basel-Binningen meteorological station (Fig. 1, 7°35′ N, 47°32′ W, MeteoSwiss, 1940). To account for more (urbanized) or less (public parks) sealed surfaces the model area was subdivided into zones (Fig. 1). For the two zones monthly running averages of cumulated daily precipitation which were reduced by a factor of 1/30 or 1/3, respectively, were introduced as groundwater recharge (see Huggenberger et al., 2006).

3.2.2 River model boundary

The river model boundary was chosen as transient Cauchy boundary condition considering daily intervals of head and river water temperature data (Fig. 1). The transfer rate (see above) for regions beneath the river corresponds to river bed conductance. The zonation of these regions corresponds to the location of the sheet pile wall at the river board as well as to the thickness of the gravel layer in the river bed, which is thickest in the south (Fig. 1).

3.2.3 Lower boundary

The lower boundary was defined by the basal heat flux of approx. $0.07\,\mathrm{W\,m^{-2}}$, which was derived from results obtained during several deep drilling projects in the region of Basel.

3.2.4 Northwestern model boundary

The northwestern model boundary was defined as: (a) no flow along a flow line extending from the southern model boundary to a step in the bedrock located in the middle of the model domain (cf. Figs. 1 and 2); and (b) transient Cauchy boundary condition with daily intervals of head extending from the step in the bedrock to the river Rhine (cf. Figs. 1 and 2). According to the progression of seasonal temperature measurements near the northwestern model boundary with minor variations (cf. OW 3, Fig. 3); no temperature exchange across this boundary was assumed.

3.2.5 Southern model boundary

The southern model boundary was defined as transient Dirichlet boundary condition for head and temperature by including daily interval data from four observation wells (Fig. 1). Temperature data from four observation wells allowed taking into account several thermal influences such as: (a) the densely urbanized area up-gradient of the middle part of the southern model boundary (cf. Fig. 1); (b) the less urbanized area up-gradient of the left side of the southern model boundary and within the southwestern part of the model domain (cf. Fig. 1); and (c) an area with little influence on the thermal groundwater regime on the right side of the southern model boundary where the thickness of the groundwater saturated zone is small.

3.2.6 Injection of water with elevated temperatures used for cooling

Detailed data of extraction and injection rates/temperatures was only available for one thermal groundwater user (Bürgerspital; Fig. 2). Additionally, two thermal groundwater users with injection of water with an assumed average temperature increase of 4 K (compared to the extracted groundwater temperature; PUK and garbage incarnation facility) were considered.

3.2.7 Thermal input of heated construction parts reaching into the groundwater (cellars, underground parking lots, etc.)

In a first step all large buildings (base area > 4000 m^2) with construction parts reaching into the groundwater were inventoried for the model area. In a next step the seasonal heating periods between fall and spring were selected based on heating degree-days (HDD). Degree-day methods allow quantifying the heating energy demands of buildings (Christenson et al., 2006). The definition of heating degree-days in this study is taken form a Swiss standard (1982):

$$\mathrm{HDD}\,(\theta_\mathrm{i}, \theta_\mathrm{th}) = m_k \sum_{k=1}^{n} (\theta_\mathrm{i} - \theta_{\mathrm{e},k}) \tag{1}$$

$m_k = 1\,\mathrm{day}$ if $\theta_{\mathrm{e},k} \leq \theta_\mathrm{th}$

$m_k = 0\,\mathrm{day}$ if $\theta_{\mathrm{e},k} > \theta_\mathrm{th}$

In Eq. (1), θ_i denotes the internal temperature, $\theta_{\mathrm{e},k}$ the daily mean external temperature (air temperature) and θ_th the threshold temperature for heating, while k stands for the day number in the year, i.e., $k \in \{1,\ldots,366\}$. With regard to internal temperature and building quality, standard values for current building stocks in Switzerland of $\theta_\mathrm{i} = 20\,^\circ\mathrm{C}$ and $\theta_\mathrm{th} = 15\,^\circ\mathrm{C}$ were assumed in this study.

3.3 Evaluation of exploitation and urbanization scenarios

The calibrated model was used for future prediction and various exploitation and urbanization scenarios. Two sets of scenarios were evaluated. The first stet of scenarios encompasses future urbanization and additional groundwater use for cooling purposes, including an examination of the efficiency of isolation measures for buildings. The scenarios focus on the simulation of: (A) new thermal groundwater use up- and down-gradient of existing thermal groundwater users and evaluation of interference of existing and new thermal groundwater users; (B) new thermal groundwater use in areas where currently no thermal use takes place; (C) urbanization and new building-parts that reach into the aquifer according to available information on development plans; and (D) the combined effect of new thermal groundwater use and future urbanization. In order to evaluate the long-term thermal impact, the 2010 data set and scenario modifications were included cyclic for a time period of 10 yr.

The second set of scenarios deals with the compensation of past thermal influences on the thermal groundwater regime in the investigation area. Therefore, targeted new groundwater uses for heating to reduce groundwater temperatures down-gradient are introduced in two different zones of the aquifer (cf. Figs. 10 and 11). In order to evaluate the long-term thermal impact, the 2010 data set and scenario modifications were included cyclic for a time period of 30 yr.

4 Results

4.1 Monitoring results – short- and long-term variation of groundwater temperatures

Analyses of groundwater temperature data demonstrate a variable annual range of groundwater temperatures and a maximum variability of up to 3 K. The variation in measured temperature data is the combined result of: (1) heat transport from the ground surface by conduction as well as by convection with water infiltrating through the unsaturated zone and into the saturated porous medium; (2) river-groundwater interaction; as well as (3) thermal influence of thermal groundwater users and urbanization.

Figure 3 shows selected time-series of groundwater temperature measurements. The data analysis of short-term and seasonal temperature development shows that numerous observation wells measure a temperature maximum in autumn to spring what can be explained by the heating period (OW 1; Figs. 1 and 3). Generally high groundwater temperatures are attributed to diffuse influence of urbanization and heated buildings parts in the subsurface and in the groundwater as well as thermal groundwater use (OW 2; Figs. 1 and 3). In less urbanized areas groundwater temperatures are comparably low and show little variation throughout the year (OW 3; Figs. 1 and 3). Several temperature measurements show little variation throughout the year what can be attributed to zones within the aquifers where hydraulic conductivities are small due to constructions that included cement injections (Epting et al., 2008a). The data analysis of long-term temperature development show that changes within seasonal cycles can be observed for several observation wells (OW 4; Figs. 1 and 3). Several temperature measurements show a positive trend within the time series (OW 3; Figs. 1 and 3). Some observation wells show a continuous rising of temperatures which may be attributed to a retarded influence of construction development (OW 5; Figs. 1 and 3).

4.2 Monitoring results – high-resolution multilevel temperature monitoring

A detailed discussion of the high-resolution multilevel temperature measurements can be found in (Epting and Huggenberger, 2012). In summary, the measured temperatures in all four observations wells are 1 K cooler than those measured in the conventional observation wells nearby. Preferential thermal propagation in more conductive coarse fluvial deposits can be observed in all four wells. Figure 3 illustrates processes of river-groundwater interaction observed in well I close to the river (cf. Fig. 1). During flood events in summer warm water infiltrates from the river and stratifies in the upper part of the aquifer. During flood events in winter cooler water infiltrates from the river and stratifies in the lower part of the aquifer.

Only in the southern observation well IV a thermal stratification is observable where less natural and anthropogenic disturbance occurs. As for the remaining observation wells no vertical thermal stratification within the groundwater saturated zone can be observed it is hypothesized, that the classical tautochrones which describe the seasonal penetration of temperature fluctuation by subsurface temperature profiles (e.g., Taylor and Stefan, 2009; Yamano et al., 2009) are not valid for groundwater saturated zones within heterogeneous gravel aquifers where high groundwater flow velocities can be observed. Here natural and anthropogenic disturbances dominate thermal groundwater

Title Page
Abstract | Introduction
Conclusions | References
Tables | Figures
◀| |▶
◀ ▶
Back | Close
Full Screen / Esc
Printer-friendly Version
Interactive Discussion

regimes. Moreover, preferential thermal propagation is very heterogeneous and intensified in more conductive coarse fluvial deposits.

4.3 Influence of groundwater users

Table 2 summarizes the daily average and maximum energy that the three existing thermal groundwater users extracted in 2010 during the operation period in summer. The energy (E_G) in kilowatts (kW) extracted by the thermal groundwater users can be calculated using the equation:

$$E_G = H \times F \times \Delta T \tag{2}$$

where H is the specific heat of water ($\mathrm{kJ\,kg^{-1}\,K^{-1}}$), F is the flow of water (well yield $\mathrm{l\,s^{-1}}$); and ΔT is the temperature reduction or increase in the heat pump (K).

During operation in summer the three thermal groundwater users extract approx. $843\,\mathrm{m^3\,d^{-1}}$. This results in a nominal geothermal energy extraction (E_G) of in total approx. 126 kW.

4.4 Results of heat-transport modeling

Figure 4 illustrates the calibration results for the multilevel groundwater observation wells I to IV. Generally, the calibration results show that average measured temperatures are represented well by the heat-transport model. For observation wells I, II and IV the differences between calculated and observed temperatures is less than 1 K throughout 2010. For observation well III the differences between calculated and observed temperatures ranges between approx. −2.5 K and approx. 3 K for 2010. Within the unsaturated zone of observation well III the differences between calculated and observed temperatures rise towards the surface. The contrary is observed in the unsaturated zone of observation well IV where the differences between calculated and observed temperatures fall towards the surface.

The model and scenario calculations are compared and validated by means of thermal budgets through defined regions, the course of down-gradient thermal plumes as well as the description of simulated temperatures, flow paths velocities (particle tracking), and thermal retardation. The simulations provide estimates of the extent, magnitude and timing of temperature increases and decreases in the subsurface. The thermal influence of heated buildings and thermal groundwater users was evaluated by selecting down-gradient mesh nodes on stream-lines. In case of nearby groundwater use the thermal influence on the extraction was evaluated.

4.4.1 Thermal groundwater regimes “present state 2010”

Figure 5 shows the groundwater thermal regimes during winter and summer 2010. For both seasons the influence of the urbanized area resulting in elevated temperatures is distinct. Down-gradient of several thermal groundwater users the effect of injected water with elevated temperatures can be observed. In the southern part of the model area the following thermal influences can be observed: (a) elevated groundwater temperatures originating from the densely urbanized area in the south (cf. Fig. 1); as well as reduced groundwater temperatures (b) in the southwestern less urbanized areas (cf. Fig. 1); and (c) in the southeastern model area where the thickness of the groundwater saturated zone is small. Comparable low temperatures originate from the western model boundary from less urbanized areas. In winter the effect of the heated buildings within the groundwater can be observed. In summer the remnant of the heating period down-gradient is recognizable. Whereas in the entire northern industrial area elevated temperatures throughout the seasons are observable.

The results show that the emission of heated buildings and the integral of thermal influence due to urbanization can be reproduced with the heat-transport model. In densely urbanized areas with low flow velocities the influence is year-round. The influence of thermal groundwater use is limited to the summer for two users and year-round for one user (Table 2). In areas with very low flow velocities, as observed in the northern industrial area, heat conduction can dominate (see below).

4.4.2 Thermal influence of heated buildings

The influence of heated buildings in the investigation area is exemplary illustrated for two single standing buildings, the "Biozentrum" and the garbage incineration facility (Figs. 1 and 2).

The emitted heat of the "Biozentrum" building is directed mainly towards the river Rhine (Fig. 5). The simulation results show, that in approx. 25 m a temperature maximum can be observed after approx. 55 d and in 75 m after approx. 75 d (Fig. 6a). This results in thermal propagation velocities of approx. 0.5 and 0.8 $\mathrm{m\,d^{-1}}$, respectively. Calculated groundwater flow velocities in this region are in the order of 1 $\mathrm{m\,d^{-1}}$ resulting in thermal retardations of 2 and 1.25, respectively. In approx. 100 m distance downgradient no influence can be observed any more. The local temperature increase in spring-time in approx. 25 m distance is in the order of 4 K and in 60 m distance in the order of 2 K.

The emitted heat of the garbage incineration facility building is taken up mainly by their own groundwater extraction located approx. 75 m down-gradient, where a temperature maximum after 55 d can be observed. This results in a thermal propagation velocity of approx. 1.4 $\mathrm{m\,d^{-1}}$. Calculated groundwater flow velocities in this region are in the order of 5 $\mathrm{m\,d^{-1}}$ resulting in a thermal retardation of 3.6. Due to the heat emission of the building the extracted groundwater is approx. 2.2 K higher compared to the uninfluenced state. As the garbage incineration facility uses the extracted groundwater for cooling, the elevated temperatures have a negative effect on the cooling capacity.

Estimated retardation factors agree well with values obtained in similar aquifer materials: ranging from 2.2 to 3.5 for a gravel and sandy aquifer (Labhart, 1988); in the order of 2.3 for glacial outwash deposits (Markle and Schincariol, 2007); in the order of 2.0 for fine sands and 2.3 for sands and gravels (Andrews and Anderson, 1979); in the order of 1.9 for the Borden sand (Molson et al., 1992); as well as 2.0 for sandy gravels (Parr et al., 1983).

Because of the sheet pile wall along the river Rhine the flow velocities within the northern industrial area are very low (C on Fig. 1). As a result, for the thermal propagation in this area, heat conduction seems to be more relevant. This hypothesis is confirmed by calculated thermal propagation velocities which are 25-fold higher compared to the flow velocities.

4.4.3 Thermal influence of groundwater use for cooling purposes

The thermal influence of groundwater use for cooling purposes in the investigation area is exemplary illustrated for two thermal groundwater users, the “Bürgerspital” and the “Implenia AG” (Figs. 1 and 2).

The thermal influence down-gradient of the injection of the thermal groundwater user “Bürgerspital” is shown in Fig. 6b. For this groundwater user high-resolution extraction/injection groundwater rates and temperatures were available. In up to 70 m distance down-gradient a thermal maximum in autumn can be observed which indicates thermal retardation. Figure 6c shows the calculated injected heat throughout the year 2010 reaching up to 124 kW in summer which corresponds well with the values in Table 2.

Down-gradient of the injection of the thermal groundwater user “Implenia AG” the measured average groundwater temperatures at the location of the extraction are in the order of 13.8 °C. It was assumed that an average increase of the thermally used water is in the order of 4 K, which results in approx. 18 °C for the injected water (Table 2). At all observations points down-gradient of the injection a temperature maximum after 95 d can be observed. In 275 m distance the emitted heat mainly is taken up by the thermal groundwater use of the garbage incineration facility down-gradient. The calculated injected heat in summer ranges from 42 to 420 MWh (12 to 120 kW) which corresponds well with the values in Table 2.

4.5 Results of scenario calculations

The derivation of a "potential natural state" under undisturbed (pre-exploitation) conditions and the evaluation of the "influence of climate change" are covered in Epting and Huggenberger (2012). The results of this work illustrate how the thermal groundwater regime developed before major urbanization of the region and without thermal groundwater use. For different regions within the investigated area residence times of thermal changes ("memory effect" of the subsurface) could be evaluated. The comparison of the modeling results from 2010 ("present state") with the "potential natural state" of the groundwater thermal regime allowed to illustrate how the different regions of the investigated GWB are already effected by temperature increases.

4.5.1 New thermal groundwater use

Figure 1 shows the locations for which the influences of new thermal groundwater users that use the extracted groundwater for cooling purposes were evaluated. Figure 7 shows the thermal influence down-gradient of a new thermal groundwater user and within the inflow area of the groundwater user Bürgerspital (Figs. 1 and 2). Groundwater temperatures down-gradient rise to values of up to 18 °C in approx. 50 m distance and up to 16 °C in approx. 140 m distance. Figure 7 also shows the thermal influence on the thermal use of the Bürgerspital, where the temperature of extracted groundwater might rise above 15 °C.

The thermal influence of several new thermal groundwater users was systematically analyzed. A new thermal equilibrium down-gradient often takes 5 to 6 yr (Fig. 7). In areas with high flow velocities the thermal equilibrium is reached within one year. Groundwater users which thermally use groundwater for cooling purposes are influenced by new thermal groundwater users which are located up-gradient.

Figure 8 shows the thermal influence down-gradient of new thermal groundwater users which can be observed in a distance up to 300 to 400 m. An exponential relationship between thermal influence and distance can be derived. However, as this relationship does not take into account the transient character and the heterogeneous character of the numerous influences on the thermal regime of the urban GWB, results should be interpreted with care.

4.5.2 Future urbanization

Figure 1 shows the locations for which new buildings with structures reaching into the aquifer were evaluated. Figure 9 illustrates the thermal influence down-gradient of new buildings within area A (Fig. 1). Groundwater temperatures down-gradient rise to values above 15 °C in approx. 65 m distance and above 12 °C in approx. 230 m distance. Figure 9 also illustrates the thermal influence with reduced heating temperatures as a result of more efficient isolation of the buildings. Seasonal temperature variations down-gradient of buildings with structures into the aquifer are reduced for both scenarios with reduced heating temperatures. However, in distances up to approx. 270 m no temperature differences between the three scenarios can be observed. Compared to the initial scenario down-gradient groundwater temperature decreases in distances up to 230 m are in the order of 1 K when reducing heating temperatures by 2 K (scenario 1). Reducing the heat emission by further 2 K would result in a total decrease of down-gradient thermal influence by approx. 2 K (scenario 2).

The thermal influence of several areas with new buildings was systematically analyzed. The thermal influence of new heated building structures reaching into the aquifer can be observed in distances up to 230 m. A new thermal equilibrium down-gradient often takes 3 years to develop (Fig. 9). In areas with high flow velocities the thermal equilibrium is reached within the same year.

In regions near the river Rhine with low flow velocities no significant thermal influence is observed down-gradient of simulated future urbanization (Fig. 8). However, groundwater temperatures locally are elevated according to the heating degree of the buildings. Figure 8 shows the exponential relationship between distance and elevated temperatures down-gradient of the various areas with new buildings. As this relationship does not take into account the transient character and the heterogeneous character of

Title Page
Abstract | Introduction
Conclusions | References
Tables | Figures
◀| |▶
◀ ▶
Back | Close
Full Screen / Esc
Printer-friendly Version
Interactive Discussion

the numerous influences on the thermal regime of the urban GWB, results should be interpreted with care.

4.6 Potential for future thermal groundwater use within the investigate GWB

4.6.1 “Cooling”

The Swiss Guidelines on Water Protection (GSchV, 2001) permits temperature differences down-gradient of thermal groundwater use of 3 K. Figure 5 shows where in the investigated GWB current groundwater temperature have increased less than 1 K, compared to a “potential natural state”. In such areas, according the GSchV, temperature increases of 2 K of the injected water during heat pump operation would be tolerated. In regard of the small size of this southwestern area and a minimum degree of efficiency discussed above only limited potential for future thermal groundwater use for cooling purposes exists. The rest of the investigated GWB already shows temperature increases that, after the Swiss regulations, would not permit further use.

4.6.2 “Heating”

On the other hand the already elevated groundwater temperatures could be used for heat extraction. Calculated volumetric total energy contents stored within the anthropogenic influenced aquifer amounts to 1.8×10^{15} to 1.9×10^{15} J for the year 2010. In comparison, calculated volumetric total energy content stored within the “potential natural” temperature aquifer amounts to only 1.4×10^{15} J. Hence, about 0.4×10^{15} to 0.5×10^{15} J are stored additionally within the anthropogenic aquifer which is equivalent to 4.6 to 5.8 GWh.

The following assumptions were made for the potential use of the urban GWB for heating: as only elevated groundwater temperatures are observed in the investigated GWB, according to Swiss Guidelines on Water Protection (GSchV, 2001), practically everywhere temperature reductions of up to 3 K down-gradient of thermal groundwater use would be feasible. Figure 5 illustrates the potential for future thermal groundwater use ("heating") for the investigated GWB and an area with already observed temperature increases of more than 4 K in winter or 5 K in summer in winter. Other important factors to be considered are flow budgets, which were calculated through a zone of the designated area and amount to 430 to 690 $m^3 d^{-1}$. Assuming a heat extraction of 5 or 8 °C would result in nominal geothermal heating resources of 112 to 128 KW and 179 to 225 kW, respectively (Table 3). Figure 10 shows the results of a scenario that is based on new thermal groundwater use for heating purposes in zone B (Fig. 1). For the simulation a temperature of the injected water of 10 °C was considered. The calculated temperature distributions illustrate the long-term development of temperatures down-gradient of the injection after 10 and 30 yr. Figure 12 (Zone B) shows the thermal influence down-gradient of the injection. After approx. 15 to 20 yr a new thermal equilibrium can be observed with temperatures ranging between 10.5 and 11.5 °C.

Figure 11 shows the results of a scenario that is based on new thermal groundwater use for heating purposes in zone C (Fig. 1) together with the location of the extraction and injection well. For the simulation a temperature of the injected water of 10 °C was considered. The calculated temperature distributions illustrate that because of the high density of heated buildings reaching into the aquifer and low groundwater flow velocities behind the sheet pile wall even under the consideration of a long-term development, groundwater temperatures in zone C are only locally reduced to temperatures between 11 and 12 °C. Figure 12 (Zone C) shows the thermal influence down-gradient of the injection. Already after 2 to 3 yr a new thermal equilibrium can be observed with temperatures between 11 and 11.5 °C. The temperature of the extracted groundwater shows a phase interference of different influences, including the heating periods of the buildings and the injection up-gradient. Extraction temperatures are very unstable and can be as low as 10 °C, which would reduce the heat extraction potential.

Title Page
Abstract Introduction
Conclusions References
Tables Figures
◀▏ ▕▶
◀ ▶
Back Close
Full Screen / Esc
Printer-friendly Version
Interactive Discussion

5 Discussion

The presented data allowed a comparison of short- and long-term temperature data with modeled groundwater temperatures. The datasets also allowed a calibration of high resolution 3-D numerical coupled groundwater flow and heat transport models. As a result, seasonal and anthropogenic influences on the temperature regime of the urban GWB in the Basel area could be distinguished.

Results of the multilevel temperature monitoring improved the interpretation of existing temperature measurements within the investigation area. The measured temperatures in all four observations wells are 1 K "colder" than those measured in the conventional observation wells nearby. It is hypothesized that this temperature difference can be explained by thermal convection within the air filled measuring tubes of the conventional observation wells.

Furthermore, no direct influence of seasonal thermal regimes originating from the ground surface could be observed within the groundwater saturated zones. Moreover, natural and anthropogenic disturbances seem to dominate thermal groundwater regimes in heterogeneous gravel aquifers where high groundwater flow velocities are observed.

Preferential thermal propagation is very heterogeneous and intensified in more conductive coarse fluvial deposits. In addition, the high-resolution vertical temperature profiling was used to study specific short-term processes and to further calibrate the numerical models. Future temperature scenarios were derived based on the calibrated heat transport model.

5.1 Effects of boundary conditions

Thermal groundwater use together with the increasing number of heated buildings that reach into the aquifer and the long-term positive trend of air and river temperatures make subsurface temperatures in the urban area of Basel higher than in surrounding rural areas.

An important GWB boundary is the river Rhine. Alongside seasonal variations the temperatures show a clear positive trend (combined impacts of climate change and anthropogenic activities within the catchment area).

Heat loss from buildings is having a noticeable influence on the distribution of subsurface temperatures in Basel. The resulting distribution of temperatures is dependent on the following factors: (1) the historical duration of heat loading; (2) the distance from a given measurement point to a building; and (3) the density of buildings in the given area. In spring after the heating period down-gradient of heated buildings an annual groundwater temperature maximum can be observed. The numerical simulation of heat loss from temperature-controlled buildings could be used to predict the resulting subsurface temperature field down-gradient. In addition, it could be demonstrated that anthropogenic thermal influences can be persistent in the subsurface (Huang et al., 2009), because rather than radiation and advection, slow conduction can play an important role in underground heat flow.

Another major thermal input to urban GWBs originates from thermal groundwater users who use groundwater for cooling purposes. Especially in summer, down-gradient of thermal groundwater users an annual temperature maximum within the groundwater can be observed. The numerical simulation can be used to predict the resulting subsurface temperature field down-gradient.

Whereas the main natural and anthropogenic impacts on the thermal groundwater regime of the GWB in the Basel area could be reproduced with the performed modeling approach, in future modeling results could be improved by: (1) recording groundwater extraction and reinjection quantities and temperatures for thermal groundwater use at least on a daily basis; and (2) introducing the effect of subsurface construction, including the sewage network, within the unsaturated zone.

5.2 Implications for urban groundwater management

The now available tools allow optimizing new locations for thermal groundwater use and urbanization (dimensioning and site evaluation of extraction and injection locations;

spatial optimal integration into existing supply networks and consideration of subsurface infrastructures) considering long- and medium-term development as well as groundwater management programs (operation schedules; temporal optimal organization of extraction and injection of groundwater).

The results from the investigated GWB allowed providing guidelines and a suitability map for geothermal subsurface use to the authorities. The suitability maps provide information on different zones within the urban GWB, where recommendations can be formulated as to what extend groundwater can be quantitatively or qualitatively used.

For the urban area of Basel the use of groundwater for heating purposes would offer an economically auspicious alternative of resource exploitation. Thereby, shallow systems could be used for cooling and deeper systems (up to 400 m) for heat storage (i.e. seasonal storage of heat in deeper geological formations). These strategies could allow compensating past and future thermal influence from urban development and climate change.

Such sustainable solutions should also include the provision of legal frameworks on the isolation of subsurface buildings and in case of new thermal groundwater use the application of balanced heating and cooling facilities.

6 Conclusions

Thermal groundwater use and the injection of water with elevated or decreased temperatures, heated buildings reaching into the aquifer and river-groundwater interactions inevitably leave their fingerprints on urban groundwater bodies. The various thermal fingerprints persist within the aquifer with characteristic extensions and life-spans resulting in a memory effect of the aquifer. To study the influence of the various thermal fingerprints and memory effects the past and future thermal development of urban groundwater bodies has to be assessed for different timescales.

For the sustainable development of urban subsurface resources, adequate management concepts are required. This includes the setup of tools that enable the investigation of the relevant processes that dominate groundwater flow and thermal regimes at different spatiotemporal scales. The extensive use of geothermal technologies is still limited, mainly because of a lack of information on the advantages and uncertainties on possible long-term environmental effects.

Acknowledgement. We thank the AUE BS for their cooperation in scope of this project.

References

Allen, A., Milenic, D., and Sikora, P.: Shallow gravel aquifers and the urban “heat island” effect: a source of low enthalpy geothermal energy, Geothermics, 32, 569–578, doi:10.1016/S0375-6505(03)00063-4, 2003.

Ampofo, F., Maidment, G. G., and Missenden, J. F.: Review of groundwater cooling systems in London, Appl. Therm. Eng., 26, 2055–2062, doi:10.1016/j.applthermaleng.2006.02.013, 2006.

Andrews, C. B. and Anderson, M. P.: Thermal alteration of groundwater caused by seepage from a cooling lake, Water Resourc. Res., 15, 595–602, 1979.

Banks, D.: Thermogeological assessment of open-loop well-doublet schemes: a review and synthesis of analytical approaches, Hydrogeol. J., 17, 1149–1155, doi:10.1007/s10040-008-0427-6, 2009.

Barrash, W., Clemo, T., Fox, J. J., and Johnson, T. C.: Field, laboratory, and modeling investigation of the skin effect at wells with slotted casing, Boise Hydrogeophysical Research Site, J. Hydrol., 326, 181–198, doi:10.1016/j.jhydrol.2005.10.029, 2006.

CEC, C. o. t. E. C.: Directive of the European Parliament and of the Council establishing a framework for Community action in the field of water policy, Joint text approved by the Conciliation Committee, Brüssel, 1997/0067(COD), C5-0347/00, 2000.

Christenson, M., Manz, H., and Gyalistras, D.: Climate warming impact on degree-days and building energy demand in Switzerland, Energ. Convers. Manage., 47, 671–686, doi:10.1016/j.enconman.2005.06.009, 2006.

Dahlem, K.-H.: The effect of groundwater on the heat loss of building parts in contact with ground, PhD, Bauphysik/Technische Gebäudeausrüstung/Baulicher Brandschutz, Kaiserslautern, 2000.

Dahlem, K.-H. and Heinrich, H.: Einfluss des Grundwassers auf den Wärmeverlust beheizter Keller, 10. Bauklimatisches Symposium, Dresden, September 1999.

Diersch, H. J. G.: FEFLOW Reference Manual, Institute for Water Resources Planning and Systems Research Ltd., Berlin, Germany, 2002.

Epting, J. and Huggenberger, P.: Unraveling the heat island effect observed in urban groundwater bodies, J. Hydrol., in review, 2012.

Epting, J., Huggenberger, P., and Rauber, M.: Integrated methods and scenario development for urban groundwater management and protection during tunnel road construction: a case study of urban hydrogeology in the city of Basel, Switzerland, Hydrogeol. J., 16, 575–591, doi:10.1007/s10040-007-0242-5, 2008a.

Epting, J., Huggenberger, P., Regli, C., Spoljaric, N., and Kirchhofer, R.: Integrated methods for urban groundwater management considering subsurface heterogeneity, in: Quantitative Information Fusion for Hydrological Sciences, edited by: Cai, X. and Jim Yeh, T.-C., Studies in Computational Intelligence, Springer Series, Berlin, Heidelberg, 183–218, 2008b.

Epting, J., Huggenberger, P., and Butscher, C.: Thermal groundwater use in urban areas, spatiotemporal scales and concepts, GQ10 Conference, Groundwater Quality Management in a Rapidly Changing World, Zürich, 13–18 June 2011.

Ferguson, G. and Woodbury, A. D.: Subsurface heat flow in an urban environment, J. Geophys. Res.-Solid Earth, 109, B02402, doi:10.1029/2003JB002715, 2004.

Florides, G., and Kalogirou, S.: Ground heat exchangers – a review of systems, models and applications, Renew Energ., 32, 2461–2478, doi:10.1016/j.renene.2006.12.014, 2007.

Fujii, H., Itoi, R., Fujii, J., and Uchida, Y.: Optimizing the design of large-scale ground-coupled heat pump systems using groundwater and heat transport modeling, Geothermics, 34, 347–364, doi:10.1016/j.geothermics.2005.04.001, 2005.

Fujii, H., Inatomi, T., Itoi, R., and Uchida, Y.: Development of suitability maps for ground-coupled heat pump systems using groundwater and heat transport models, Geothermics, 36, 459–472, doi:10.1016/j.geothermics.2007.06.002, 2007.

GSchV: Gewässerschutzverordnung, Schweizerischer Bundesrat, Bern, 2001.

Haehnlein, S., Bayer, P., and Blum, P.: International legal status of the use of shallow geothermal energy, Renew Sust. Energ. Rev., 14, 2611–2625, doi:10.1016/j.rser.2010.07.069, 2010.

Hassanizadeh, S. M.: Modeling species transport by concentrated brine in aggregated porous-media, Transport Porous Med., 3, 299–318, 1988.

Huang, S. P., Taniguchi, M., Yamano, M., and Wang, C. H.: Detecting urbanization effects on surface and subsurface thermal environment – a case study of Osaka, Sci. Total Environ., 407, 3142–3152, doi:10.1016/j.scitotenv.2008.04.019, 2009.

Huggenberger, P. and Epting, J.: Urban Geology – Process-Oriented Concept for Adaptive and Integrated Resource Management, Springer, Basel, 2011.

Huggenberger, P., Epting, J., Spottke, I., Regli, C., and Zechner, E.: INTERREG III A-Projekt MoNit "Modellierung der Grundwasserbelastung durch Nitrat im Oberrheingraben", Landesanstalt für Umwelt, Messungen und Naturschutz Baden-Württemberg, Teilprojekte Nitratherkunft (Nitrat-Transportmodellierung) und Fluss-Grundwasser-Interaktion (regionale hydrologische Grundlagendaten), Landesamt für Umwelt, Messungen und Naturschutz Baden-Württemberg, Karlsruhe, 110 pp, 2006.

Kalogirou, S. and Florides, G.: Ground heat exchangers – a review of systems, models and applications, Renew Energ., 32, 2461–2478, doi:10.1016/j.renene.2006.12.014, 2007.

Labhart, W.: Beispiel einer thermischen und chemischen Beeinflussung des Grundwassers durch Einleitung von erwärmten Wasser (Sarnen/Kanton Obwalden), PhD, ETH, Zürich, 1988.

Lever, D. A. and Jackson, C. P.: On the equations of concentrated salt solution through porous medium, US Department of Energy, Report No. DOE/RW/85.100 1985.

Mallet, J. L.: Discrete smooth interpolation in geometric modeling, Computer-Aided Design, 24, 178–191, 1992.

Mallet, J. L.: Geomodeling, Oxford University Press, New York, 2002.

Markle, J. M. and Schincariol, R. A.: Thermal plume transport from sand and gravel pits – potential thermal impacts on coot water streams, J. Hydrol., 338, 174–195, doi:10.1016/j.jhydrol.2007.02.031, 2007.

Markle, J. M., Schincariol, R. A., Sass, J. H., and Molson, J. W.: Characterizing the two-dimensional thermal conductivity distribution in a sand and gravel aquifer, Soil Sci. Soc. Am. J., 70, 1281–1294, doi:10.2136/sssaj2005.0293, 2006.

Molson, J. W., Frind, E. O., and Palmer, C. D.: Thermal-energy storage in an unconfined aquifer. 2. Model development, validation, and application, Water Resourc. Res., 28, 2857–2867, 1992.

Otto, R.: Zur Bestimmung von Wärmeleitfähigkeiten der oberflächennahen Lockergesteinsschichtenfolge in Norddeutschland, Jahrestagung der DGG in Bochum, RU Bochum, 73, 2010.

Parr, A. D., Molz, F. J., and Melville, J. G.: Field determination of aquifer thermal-energy storage parameters, Ground Water, 21, 22–35, 1983.

Pouloupatis, P. D., Florides, G., and Tassou, S.: Measurements of ground temperatures in Cyprus for ground thermal applications, Renew Energ., 36, 804–814, doi:10.1016/j.renene.2010.07.029, 2011.

SIA: Heating degree-days in Switzerland, Swiss Association of Engineers and Architects, Standard 381/3, 1982.

Shi, B., Liu, C., Wang, B. J., and Zhao, L. Z.: Urban heat Island effect on engineering properties of soil and the related disaster effect, Adv. Earth Sci., 23, 1167–1173, 2008.

Spitler, J. D.: Ground-source heat pump system research – past, present, and future, Hvac&R Res., 11, 165–167, 2005.

Taniguchi, M., Shimada, J., Tanaka, T., Kayane, I., Sakura, Y., Shimano, Y., Dapaah-Siakwan, S., and Kawashima, S.: Disturbances of temperature-depth profiles due to surface climate change and subsurface water flow: 1. An effect of linear increase in surface temperature caused by global warming and urbanization in the Tokyo metropolitan area, Japan, Water Resourc. Res., 35, 1507–1517, 1999.

Taniguchi, M., Ishitobi, T., Burnett, W. C., and Wattayakorn, G.: Evaluating ground water-sea water interactions via resistivity and seepage meters, Ground Water, 45, 729–735, doi:10.1111/j.1745-6584.2007.00343.x, 2007.

Taylor, C. A. and Stefan, H. G.: Shallow groundwater temperature response to climate change and urbanization, J. Hydrol., 375, 601–612, doi:10.1016/j.jhydrol.2009.07.009, 2009.

Yamano, M., Goto, S., Miyakoshi, A., Hamamoto, H., Lubis, R. F., Monyrath, V., and Taniguchi, M.: Reconstruction of the thermal environment evolution in urban areas from underground temperature distribution, Sci. Total Environ., 407, 3120–3128, doi:10.1016/j.scitotenv.2008.11.019, 2009.

Zhu, K., Blum, P., Ferguson, G., Balke, K. D., and Bayer, P.: The geothermal potential of urban heat islands, Environ. Res. Lett., 5, 044002, doi:10.1088/1748-9326/5/4/044002, 2010.

Zhu, K., Blum, P., Ferguson, G., Balke, K. D., and Bayer, P.: The geothermal potential of urban heat islands, Environ. Res. Lett., 6, 019501, doi:10.1088/1748-9326/6/1/019501, 2011.

Table 1. Thermal material properties selected for the heat transport model.

Parameter	
Volumetric heat capacity of the gravel c_s ($\mathrm{J\,m^{-3}\,K^{-1}}$)	2.87×10^6
Thermal conductivity of the gravel λ_s ($\mathrm{J\,m^{-1}\,s^{-1}\,K^{-1}}$)	2.70
Volumetric heat capacity of water c_w ($\mathrm{J\,m^{-3}\,K^{-1}}$)	4.20×10^6
Thermal conductivity of water λ_w ($\mathrm{J\,m^{-1}\,s^{-1}\,K^{-1}}$)	6.00×10^{-1}
Longitudinal dispersivity αL (m)	20
Transversal dispersivity αT (m)	2
Transfer rate from the surface to the river bed (In/Out) ($\mathrm{J\,m^{-2}\,d^{-1}\,K^{-1}}$) T_r (–)	1.25×10^4

Title Page
Abstract | Introduction
Conclusions | References
Tables | Figures
◀I | ▶I
◀ | ▶
Back | Close
Full Screen / Esc
Printer-friendly Version
Interactive Discussion

Table 2. Energy extracted for cooling by thermal groundwater users for 2010 (see Fig. 1 for locations of thermal users).

Thermal groundwater user Operation period (d)	Well yield ($m^3\,d^{-1}$) Average (maximum)	Temperature reduction (K) Average (maximum)	Energy extracted (kW) Average (maximum)
Bürgerspital (83–318)	512 (1002)	2 (3) measured	52 (126)
Implenia AG (91–334)	231 (1305)	4*	55 (254)
PUK (1–365)	100 (218)	4*	19 (33)
Sum	843 (2525)	–	126 (413)

* Estimated (see text).

Title Page
Abstract | Introduction
Conclusions | References
Tables | Figures
◀| |▶
◀ ▶
Back | Close
Full Screen / Esc
Printer-friendly Version
Interactive Discussion

Table 3. Calculated nominal low enthalpy geothermal heating resources for zone B (see Fig. 1 for locations of new thermal groundwater users).

Well yield ($m^3\,d^{-1}$)	Groundwater temperature (°C)	Temperature reduction in the heat pump (K)	Nominal geothermal heating resource (kW)
430–520 (summer)	15	5	112–124
		8	179–198
600–690 (winter)	14	4	115–128
		7	201–225

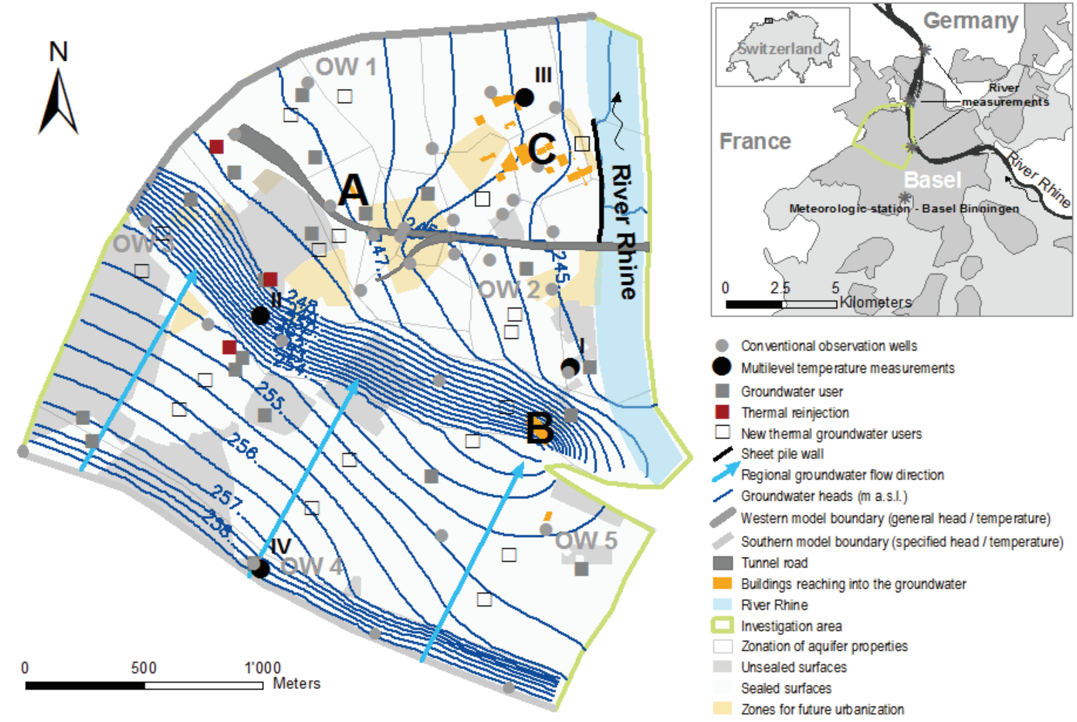

Fig. 1. (Caption on next page.)

Title Page
Abstract
Introduction
Conclusions
References
Tables
Figures
◀◀
▶▶
◀
▶
Back
Close
Full Screen / Esc
Printer-friendly Version
Interactive Discussion

Fig. 1. Study area in the agglomeration of Basel, including model boundary conditions for flow and heat-transport. OW1-5: Data from conventional observation wells used for discussion. I–IV: Locations of multilevel temperature measurements. A: Garbage incarnation facility; B: Biozentrum; and C; Northern industrial area. Also shown is the regional groundwater flow regime with the main flow directions. Note the steep hydraulic gradient in the center of the modeling domain resulting from the progression of the bedrock (cf. Fig. 2) and the backwater effects along the tunnel road and sheet pile wall.

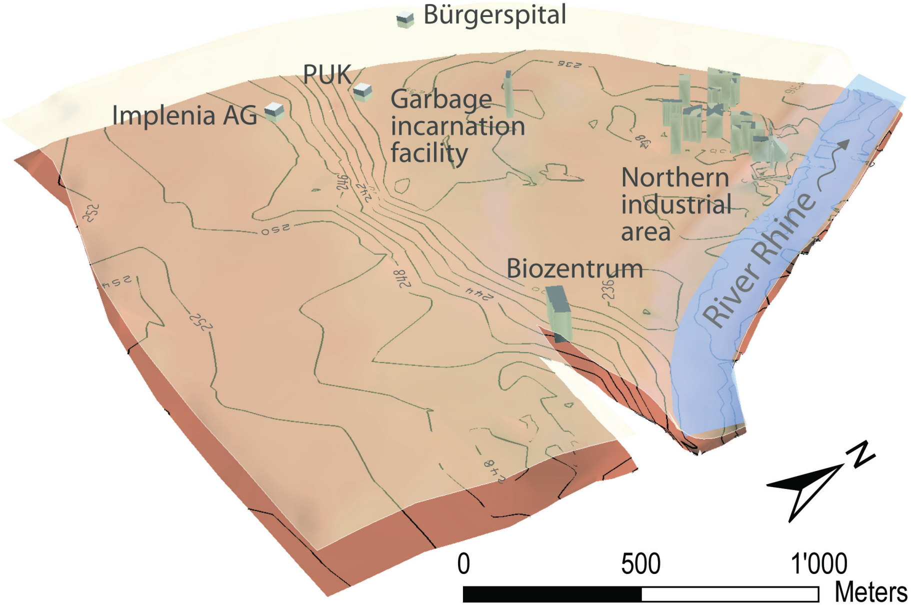

Fig. 2. 3-D-GWB of the modeled area illustrated together with building parts (dark grey) that reach into the groundwater and thermal groundwater users (grey cubes). The upper surface shows the topography of the land surface. The lower surface shows the topography of the bedrock including a steep slope in the center of the modeling domain.

Title Page
Abstract | Introduction
Conclusions | References
Tables | Figures
◄| |►
◄ ►
Back | Close
Full Screen / Esc
Printer-friendly Version
Interactive Discussion

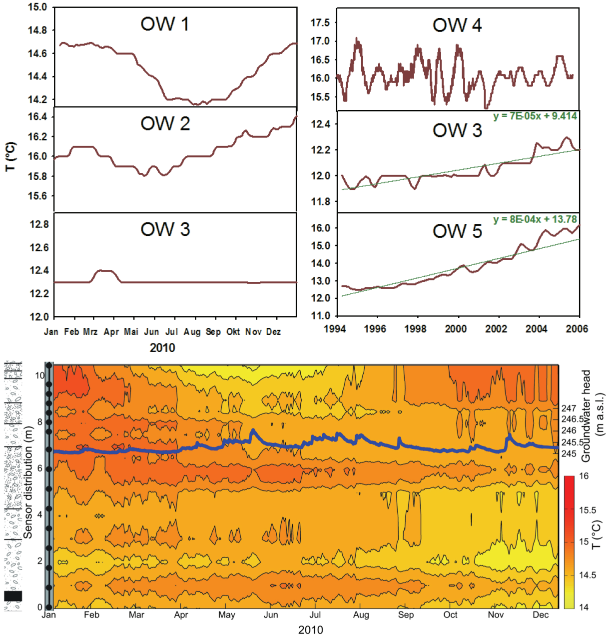

Fig. 3. Upper left: selected time-series for the year 2010 illustrating the short-term and annual development of groundwater temperatures (note the different axis intercepts; see text for further explanation and for locations Fig. 1). upper right: Selected time-series for the years 1994 to 2006 illustrating the long-term and seasonal development of groundwater temperatures (note the different axis intercepts; see text for further explanation and for locations Fig. 1). Below: temperature contour lines for 2010 based on the multilevel observation well measurements near the river Rhine (well I on Fig. 1) including groundwater head measurements (blue line) in a nearby observation well. The left axis shows the distribution of temperature sensors in 0.5 and 1 m intervals (the lowermost sensor lies 0.5 m above the bedrock). The lithostratigraphic drill-core information (left) illustrates sandy (coarse signature) and silty (fine signature) gravel sequences as well as a sandstone layer (black signature) (Huggenberger and Epting, 2011).

Title Page
Abstract | Introduction
Conclusions | References
Tables | Figures
◀| |▶
◀ ▶
Back | Close
Full Screen / Esc
Printer-friendly Version
Interactive Discussion

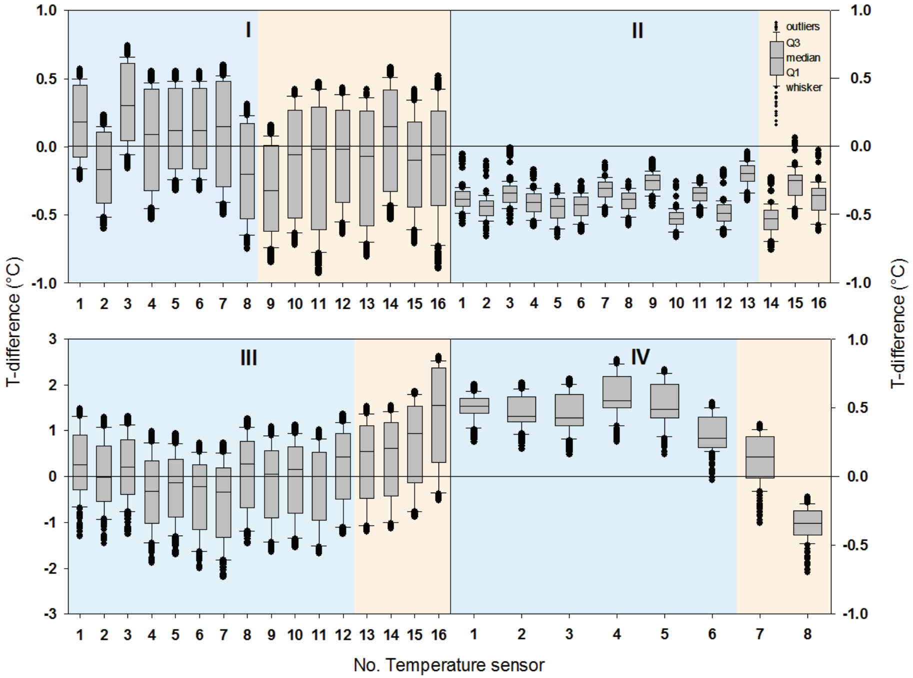

Fig. 4. Calibration results for the multilevel groundwater observation wells I–IV (for locations see Fig. 1). Observation wells I to III consist of in total 16 and observation wells IV of in total 8 temperature sensors (cf. Fig. 3). The box plots show (see also imbedded sketch upper right) the median (horizontal line within the grey shaded box), the quartiles Q1 and Q3 (shaded box), the upper and lower whiskers (horizontal bars outside of the box) as well as extreme outliers beyond the whiskers. Whiskers mark those values which are minimum and maximum unless these values exceed 1.5 times the inter quartile range (distance between Q1 and Q3). Light blue: temperature sensors located within the saturated zone; beige: temperature sensors located within the unsaturated zone. Note the different axis intercepts for observation well III.

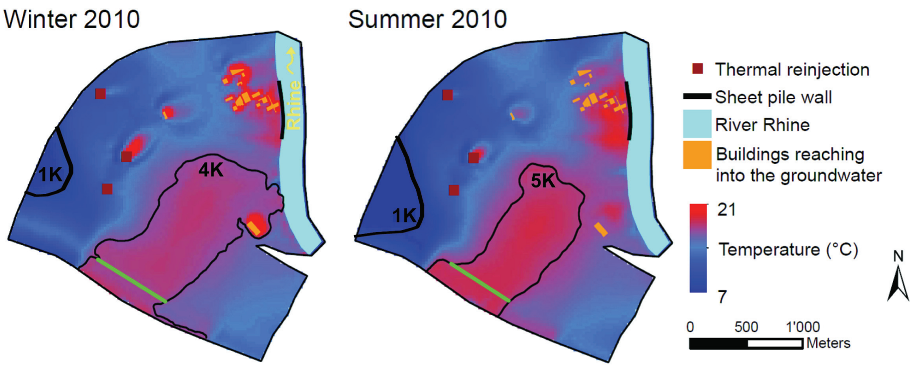

Fig. 5. Calculated temperature distribution for winter (left) and summer 2010 (right). Delineation of areas with temperature increases of < 1 K (winter and summer) as well as > 4 K (winter) and > 5 K (summer) compared to a "potential natural" state (for explanation refer to the text). Water budgets were calculated through the green zone.

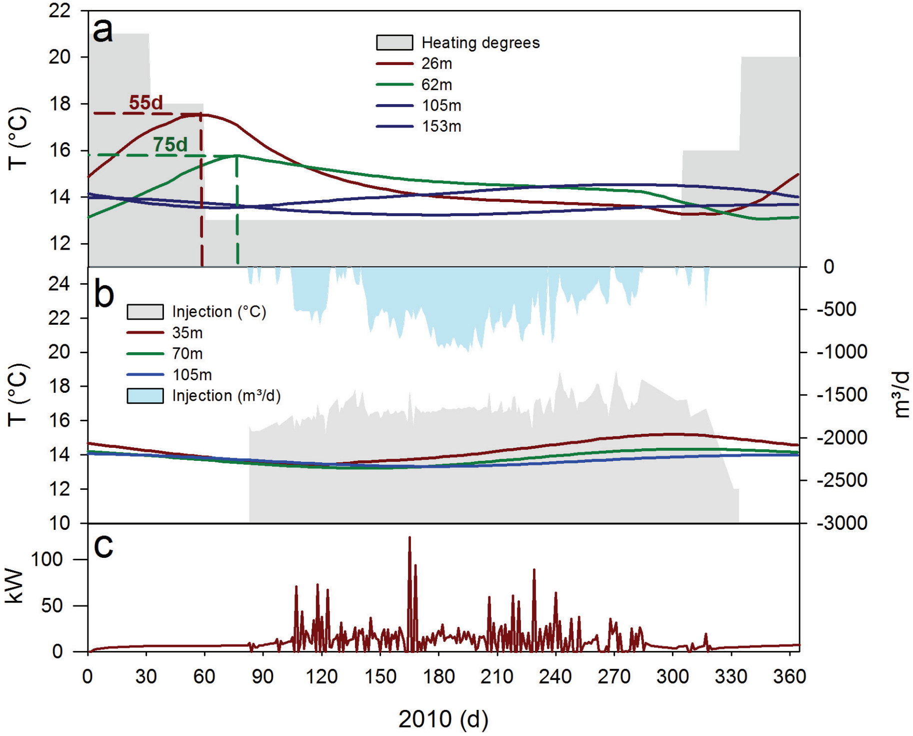

Fig. 6. Evaluation of thermal impacts to the GWB for the year 2010. **(a)** Down-gradient influence of the heated Biozentrum-building (for locations see Figs. 1 and 2) illustrated together with heating degrees for the winter heating periods 2009/2010 and 2010/2011 (for explanation refer to the text). **(b)** Down-gradient influence of the thermal groundwater user Bürgerspital who uses the extracted groundwater for cooling purposes (for locations see Figs. 1 and 2), illustrated together with injection temperatures (grey signature and left axis) and recharge (blue signature and right axis). **(c)** Calculated injected energy of the thermal groundwater user Bürgerspital.

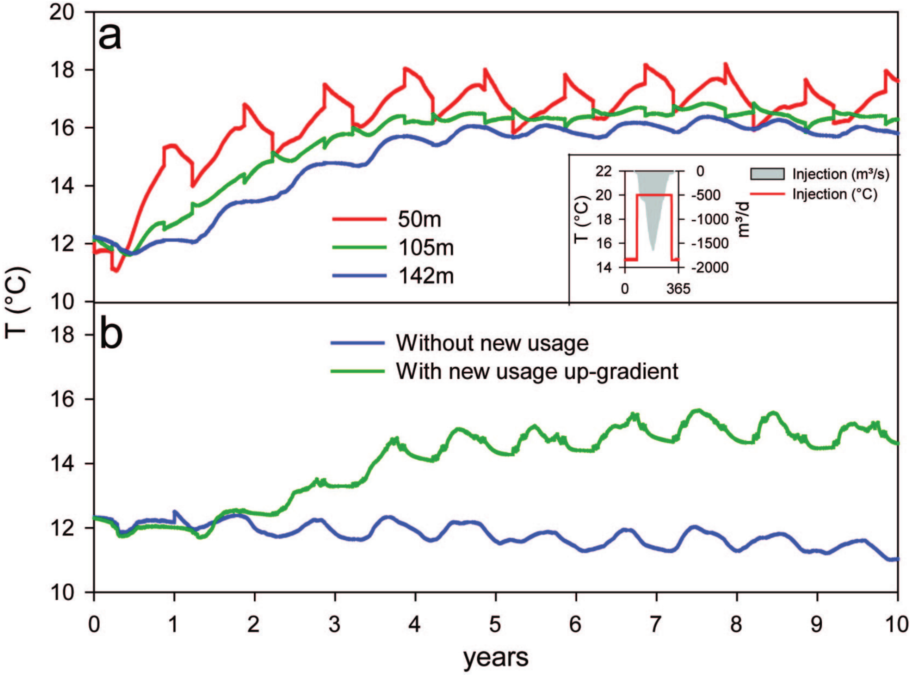

Fig. 7. Simulation of new thermal groundwater use up-gradient of the groundwater user Bürgerspital who uses the extracted groundwater for cooling purposes (for locations see Figs. 1 and 2). **(a)** Thermal influence down-gradient of the new thermal groundwater user (imbedded subplot: simulated extraction and injection rates as well as temperatures of the injected water). **(b)** Influence of the new thermal groundwater use on the thermal groundwater user Bürgerspital.

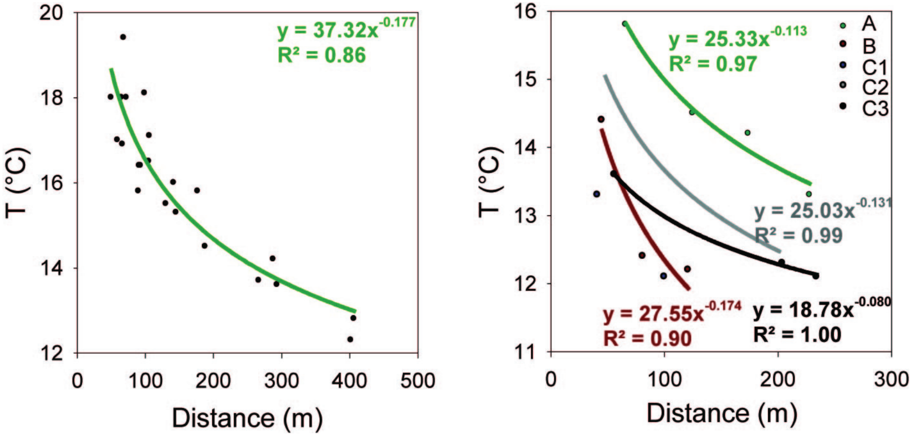

Fig. 8. Thermal influence down-gradient of simulated thermal groundwater users (left) and new buildings developed (for locations see Fig. 1).

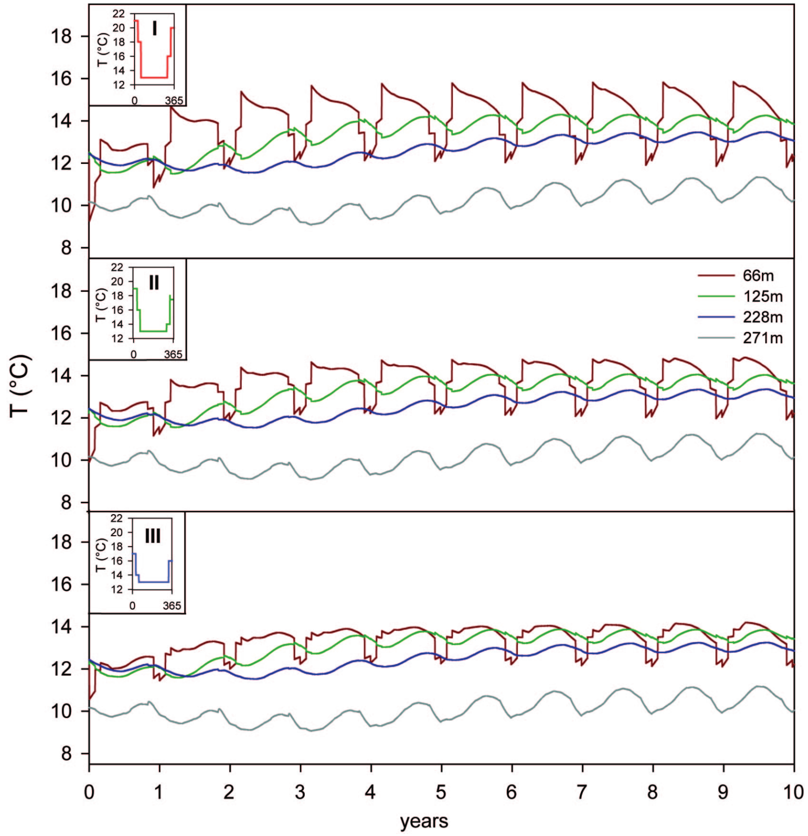

Fig. 9. Thermal influence of buildings developed in area A (for locations see Fig. 1) for different heating temperatures. Simulated heating period with: I as the standard scenario; II and III with reduced heating temperatures as a result of more efficient isolation of buildings (imbedded subplots: simulated building temperatures during heating periods).

Title Page
Abstract
Introduction
Conclusions
References
Tables
Figures
◀I
▶I
◀
▶
Back
Close
Full Screen / Esc
Printer-friendly Version
Interactive Discussion

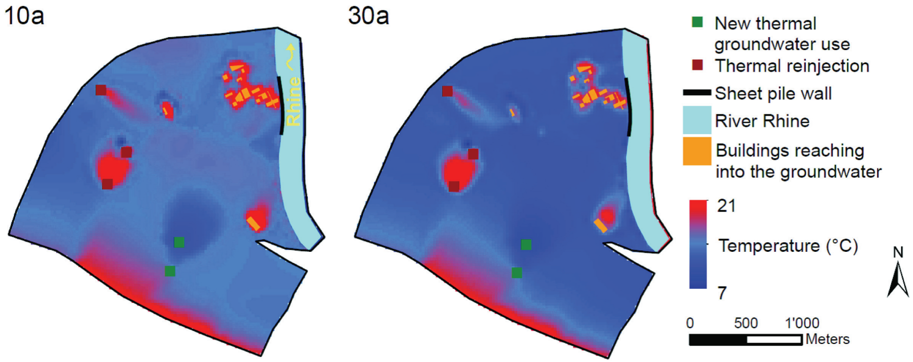

Fig. 10. Calculated temperature distribution with new groundwater use for heating after 10 yr (left) and 30 yr (right) in Zone B (for locations see Fig. 1).

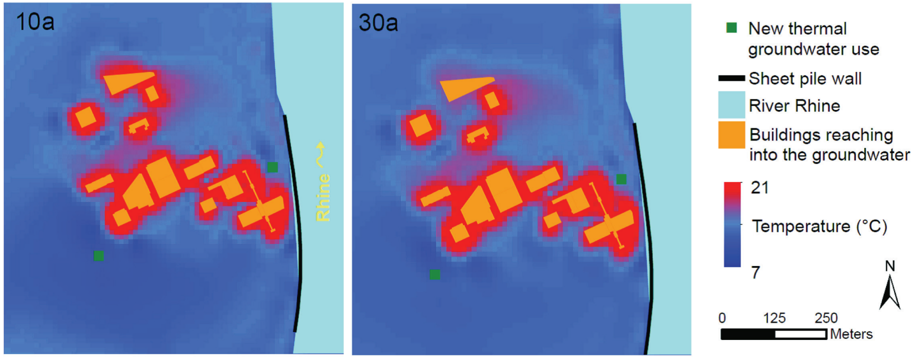

Fig. 11. Calculated temperature distribution with a new groundwater use for heating after 10 yr (left) and 30 yr (right) in Zone C (for locations see Fig. 1).

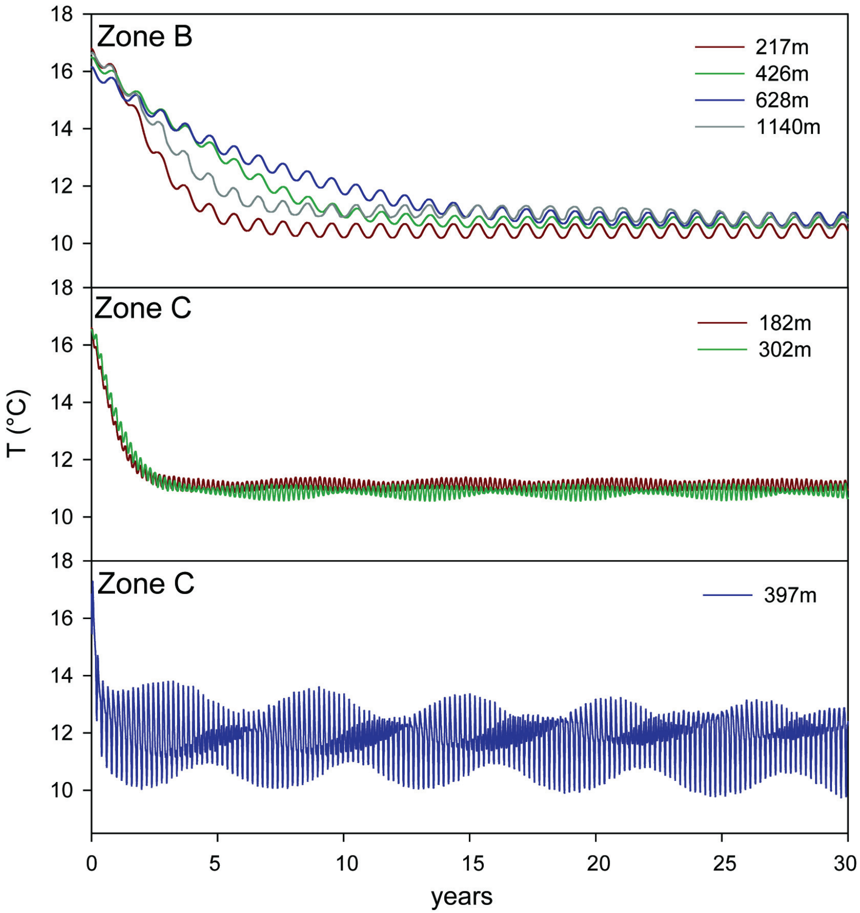

Fig. 12. Development of temperatures down-gradient of new groundwater use for heating for zones B and C (for locations see Figs. 1, 10 and 11).